TABLE III

CHARACTERISTICS OF THE NMSR CRITICAL ASSEMBLY

Fuel material	UO_2 fuel rods (swaged)
Fuel density	9.45 g/cm³
Fuel enrichment	4.0% (by weight)
Diameter of oxide	0.444 in.
Cladding material	304 stainless steel
Outside diameter of cladding	0.500 in.
Thickness of cladding	0.028 in.
Fuel length	66.7 in.
Moderator	Light water
Fuel pitch (square)	0.663 in.

A comparison of similar samples measured in the two reactors shows good agreement for the $\frac{1}{4}$-cm thick samples, but for thicker samples, the Maritime reactor shows larger reactivity changes. Since most of the samples are thermally black (see Table II for values of Σ_a times thickness), the larger reactivity effect in the NMSR reactor is most probably due to a larger fraction of epithermal absorptions. This would imply a harder spectrum for the NMSR reactor.

Table II shows reactivity data measured with samples other than rare earths in comparison with the rare earth samples. Reactivity of these samples is expressed in cents as obtained directly from the reactor periods.

Table III lists some of the characteristics of the NMSR Critical Assembly.

REFERENCE

1. H. F. JOHNSTON, J. L. RUSSELL, JR., AND W. L. SILVERNAIL, Relative control rod worth of some rare earth oxides. *Nuclear Sci. and Eng.* **6**, 93 (1959).

J. HARRY MORTENSON
RUSSELL M. BALL

The Babcock & Wilcox Company
Atomic Energy Division
Critical Experiment Laboratory
Lynchburg, Virginia

Received June 13, 1960

Comparison of Measurements with a Monte Carlo Calculated Spatial Distribution of Resonance Neutron Capture in a Uranium Rod

A recent article in this Journal (*1*) presented a comparison of measured and Monte Carlo calculated spatial distributions of resonance neutron capture across a gold rod. This letter reports a similar comparison for the case of U^{238} resonance neutron capture in a 0.387-in. diameter uranium metal rod in a hexagonal light-water moderated lattice with rod center-to-center spacing of 0.567 in.

A Monte Carlo digital program (*2*) was used to calculate the histories of 30,000 neutrons from 10 kev to 3 ev. The initial source was chosen by assuming a spatially flat, isotropic, $1/E$ flux in the cell at energies above 10 kev. Doppler broadened resonance cross sections of 27 resolved resonances were used over the energy range from 3 ev to 531 ev. Scattering was taken to be isotropic in the center-of-mass system, and interference between resonance and potential scattering was accounted for. Above 531 ev, the resonances were treated statistically, using a Porter-Thomas distribution of reduced neutron widths. The resonances were assumed to be evenly spaced with a separation of 16 ev and to have a constant $\Gamma\gamma$ of 0.024 ev. The cross-sectional area of the uranium rod was divided in the calculations into two main regions with outer radii of 0.1835 in. and 0.1935 in., respectively. Each of these two regions was subdivided into 10 equal area rings. The following calculational results were obtained:

TABLE I

NEUTRON CAPTURES[a]

ΔE (ev)	Outer region	Inner region
3.0–8.44	0.02272	0.06023
8.44–15.6	0.00055	0.00485
15.6–28.9	0.01062	0.03179
28.9–51.6	0.00840	0.03002
51.6–73.7	0.00317	0.01160
73.7–85.6	0.00109	0.00439
85.6–96.5	0.00013	0.00111
96.5–110.0	0.00247	0.00888
110.0–131.5	0.00184	0.00511
131.5–156.0	0.00037	0.00195
156.0–178.5	0.00057	0.00260
178.5–201.0	0.00111	0.00500
201.0–381.5	0.00337	0.01348
381.5–539.0	0.00141	0.00760
539.0–2000	0.00561	0.02937
2000–10000	0.00316	0.02293
Total/region	0.06659	0.24091
Inner region		0.24091
Outer region		0.06659
Total capture		0.30750

[a] Normalized to one neutron entering at 10 kev.

1. Fraction of neutrons started at 10 kev which are captured in the uranium rod above 3 ev.
2. Fraction of total capture in each of the twenty rings across the uranium rod.
3. Fraction of total capture in each of 16 energy intervals for each of the two main regions.

From the Monte Carlo calculations, a resonance escape probability (P) of 0.693 was obtained, which gave an effective resonance integral of 10.65 barns. To obtain the complete resonance integral above 0.5 ev, 1.3 barns (*3*, *4*) is added to account for p wave capture up to 30 kev and s wave capture from 10 to 30 kev. Also, 0.8 barns is added for all capture above 30 kev. There is 0.7 barn of $1/v$ capture between 0.5 ev and 3 ev; most of the remaining 0.5 barn of $1/v$ capture is accounted for by the Monte Carlo calculation. Therefore, 0.8 barns is added to account for $1/v$ capture.

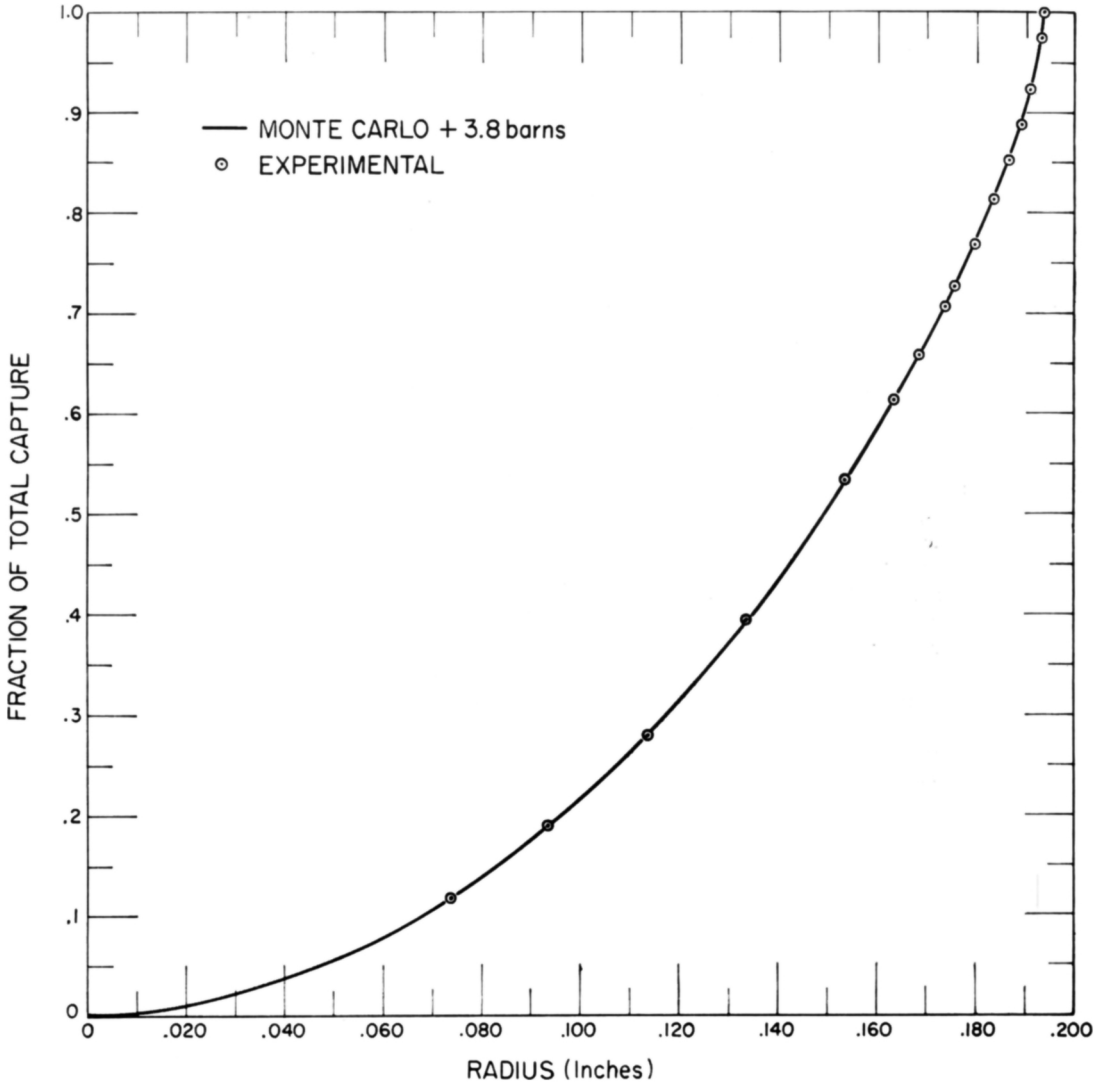

FIG. 1

This value is not in error by more than 0.2 barn. In addition, 1.2 barns is added to account for capture due to the high energy flux peak (in excess of $1/E$) in our hydrogen moderated reactor. Thus a total of 4.1 barns should be added as unshielded capture to the Monte Carlo results. The actual best fit to the experimental data was found by adding 3.8 ± 0.5 barns to the Monte Carlo results, which is not in disagreement with the expected value of 4.1 barns. Table I lists the calculated capture fractions as a function of energy for each of the two main regions.

The spatial distribution of U^{238} resonance neutron capture was measured by stacking 0.001-in. uranium foils depleted to 190 ppm U^{235}, in a hole drilled across the diameter of the uranium rod (*5*). The distribution was carried to the surface of the rod by means of 1 mg/cm^2 deposits of U_3O_8 on 0.001-in. aluminum foils placed at the rod center and against the rod surface. The foil assembly was encapsulated in 0.020 inches of cadmium. The deposits and foils were γ counted on a NaI scintillation spectrometer. An uncertainty of about 1% is assigned to each measured point of the spatial distribution.

Figures 1 and 2 show the comparison of the adjusted Monte Carlo calculation with the measured spatial distribution. Figure 1 is an integral plot showing the fraction of total capture within a radius r.

Figure 2 is a differential plot showing the measured spatial distribution of resonance neutron capture per U^{238} atom and the Monte Carlo results with 3.8 barns of unshielded capture added. The two curves have been normalized to 1.0 at the center of the rod. It should be noted that near the surface of the rod where the capture is changing rapidly with radius, the Monte Carlo calculation follows the experimental curves quite well.

The results presented indicate that the code used is quite capable of giving a detailed prediction of the spatial distribution of resonance neutron capture across the diameter of a uranium rod. In addition, it is significant to note that the agreement between experiment and calculation

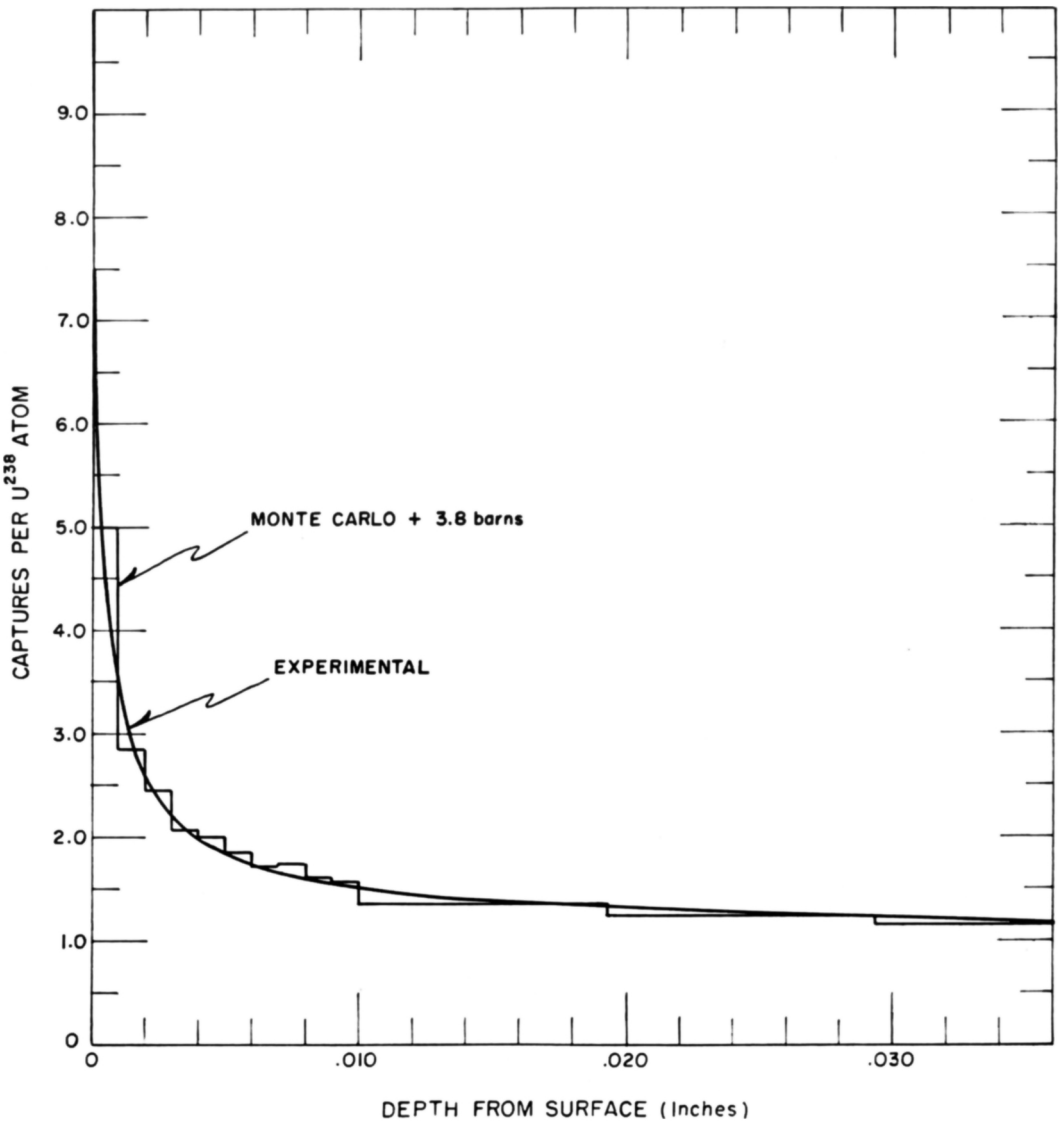

FIG. 2

gives added justification to the treatment of the higher energy resonances.

REFERENCES

1. J. HARDY, JR., G. G. SMITH, AND D. KLEIN, Resonance capture in a gold rod. *Nuclear Sci. and Eng.* **7**, 263–267 (1960).
2. R. D. RICHTMYER, R. VANNORTON, AND A. WOLFE, The monte carlo calculation of resonance capture in reactor lattices. *Proc. 2nd. Intern. Conf. Peaceful Uses Atomic Energy, Geneva, 1958* P/2489 (1958).
3. W. ROTHENSTEIN, Collision probabilities and resonance integrals for lattices. *Nuclear Sci. and Eng.* **7**, 162–171 (1960).
4. J. CHERNICK AND R. VERNON, Some refinements in the calculation of resonance integrals. *Nuclear Sci. and Eng.* **4**, 649–669 (1958).
5. D. KLEIN, W. BAER, AND G. G. SMITH, Spatial distribution of U^{238} resonance neutron capture in uranium metal rods. *Nuclear Sci. and Eng.* **3**, 698–706 (1958).

G. SMITH
J. HARDY, JR.
D. KLEIN

Bettis Atomic Power Laboratory
Westinghouse Electric Corporation
Pittsburgh, Pennsylvania

Received July 18, 1960

Some Series Occurring in the Theory of the Square Lattice Cell

Cohen (*1*), Newmarch (*2*), and other authors have calculated the flux and thermal utilization in a square lattice cell: this work is of continuing interest because of its close